JOURNAL OF MAGNETIC RESONANCE **129,** 74–84 (1997)
ARTICLE NO. MN971233

A Simple Matrix Formalism for Spin Echo Analysis of Restricted Diffusion under Generalized Gradient Waveforms

Paul T. Callaghan

Department of Physics, Massey University, Palmerston North, New Zealand

Received February 20, 1997; revised July 30, 1997

A simple mathematical formalism is presented which allows closed form expressions for the echo attenuation, $E(q)$, in spin echo diffusion experiments, for practically all gradient waveforms and for the case of restricted diffusion in enclosing pores, with or without wall relaxation. The method, which derives from the multiple propagator approach of A. Caprihan *et al.* (1996, *J. Magn. Reson. A* 118, 94), depends on the representation of the gradient waveform by a succession of sharp gradient impulses. It leads to $E(q)$ being expressed as a product of matrix operators corresponding quite naturally to the successive sandwich of phase evolution and Brownian migration events. Simple expressions are given for the case of the finite width gradient pulse PGSE experiment, the CPMG pulse train used in frequency-domain modulated gradient spin echo NMR, and the case of a sinusoidal waveform. The finite width gradient pulse PGSE and CPMG pulse trains are evaluated for the case of restricted diffusion between parallel reflecting planes. The former results agree precisely with published computer simulations while the latter calculation provides useful insight regarding the spectral density approach to impeded Brownian motion. © 1997 Academic Press

INTRODUCTION

The pulsed gradient spin echo (PGSE) experiment (*1*) provides a means to encode the spin phase distribution for translational motion in a manner which enables the echo attenuation to be used to elucidate particle dynamics. In particular, for restricted particle motion it has been shown (*2*) that the echo attenuation can be interpreted in terms of a scattering theory where the scattering wave vector, $\mathbf{q}$, is identified with the gradient pulse area. As a result the Fourier spectrum of the confinement space appears explicitly in the measurement (*3*), an effect which has been termed diffusive diffraction (*2, 4, 5*). This q-space diffraction approach has been used by a number of authors (*4–13*) to examine morphological characteristics at length scales smaller than those which can normally be accessed using conventional NMR microscopy.

One of the central problems in PGSE q-space diffraction experiments concerns the reliance of the scattering formalism on an approximation of the gradient waveform by two narrow pulses. In particular, it is assumed that not only is the duration δ of the pulses much smaller than their separation Δ but that the distance diffused during the pulses is small compared with characteristic dimensions of the pore space morphology. Because the wave vector amplitude q depends on the time integral of the pulse, this restriction to narrow pulses represents a constraint on the maximum available scattering wave vector. Furthermore the need to ensure that the diffusion distance is small during the pulses further constrains the distance scales which can be probed using this experiment. In consequence it would be helpful to find a convenient mathematical treatment which is applicable to the case of finite pulse durations. An additional reason to consider such a treatment concerns applications where the applied gradient is constant, for example, as in stray field experiments. Consequently a number of authors have recently addressed the issue of q-space diffraction under conditions of finite gradient pulse widths, both in qualitative terms (*14*) and by means of computer simulation (*6, 15*). A significant and successful analytic treatment of the finite pulse problem has been demonstrated by Caprihan *et al.* (*16*). The success of their method has acted as an encouragement to simplify their approach, and to express the underlying mathematics in a readily understandable formalism.

Before proceeding it is important to appreciate that there exist other classes of experiments to which such a simple formalism might be usefully applied, and in particular we will seek to find a method which is applicable to general gradient waveforms. One obvious example to be considered is the case where the gradient pulse rise time is finite or where the gradient coil is tuned to resonate in order to maximize the available gradient strength so that the relevant waveform shape is that of a sinusoid. And, quite apart from the two-gradient-pulse PGSE experiment, there has been a demonstration recently of a very different form of generalized modulated gradient spin echo experiment in which a periodic gradient waveform is used. In these frequency domain modulated gradient spin echo (FD-MGSE) measurements (*17, 18*), one samples molecular dynamics in the frequency domain rather than in the time domain. For such a class of experiments the waveform is designed so that the

1090-7807/97 $25.00

time integral of the effective gradient has well-defined frequency characteristics. The FD-MGSE method has been shown to provide access to much shorter time scales than that of the traditional two-pulse PGSE experiment.

The original theory for the FD-MGSE experiment was developed by Stepisnik (*19, 20*) who used a translational motion spectral density approach, directly analogous to the measurement of rotation motion spectral density in T_1 dispersion experiments. However this theory relies on a Gaussian moment assumption, an unsatisfactory condition when the motion is restricted. Recently, Stepisnik has extended his original treatment to allow for the effects of restricted diffusion (*21*). It is the purpose of the present article to demonstrate a very different but also completely general approach to modulated gradient spin echo NMR which can work for any gradient waveform and for any morphological characteristics associated with restricted diffusion, with or without spin relaxation at boundary surfaces. As we shall show, the method of calculation is both simple and intuitive.

A number of historical formalisms are available (*2*) for the interpretation of the echo amplitude when the molecular motion under consideration is unrestricted Brownian self-diffusion and the distribution of molecular displacements is inherently Gaussian. These include the random jump model of Carr and Purcell (*22, 23*), the Bloch–Torrey equation (*24*), and the spectral density approach of Stepisnik (*20*) referred to in the previous paragraph. We shall however focus on the method of propagators, first introduced by Stejskal (*25*) and used so successfully to explain diffusive diffraction in the case of the narrow, two-pulse PGSE experiment. This propagator approach, which has been extended by Caprihan *et al.* so as to deal with multiple time steps (*16*), will form the basis of the formalism to be developed in this paper.

IMPULSE-PROPAGATOR THEORY

The basic pulse scheme for the two-pulse PGSE experiment is shown in Fig. 1 where the gradient is applied as two narrow impulses of amplitude $\mathbf{G}$, duration δ, and time separation Δ. Notice that in the case of generalized gradient and RF pulse trains, we shall find it convenient to speak of an effective gradient $\mathbf{g}(t)$ such that the effect of phase-inverting 180° RF pulses can be mimicked by simply using gradient pulses of opposite sign (while the effect of 90° RF pulses is to switch the gradient off). The point is illustrated in the simplest possible sequence shown in Fig. 1.

For the two-impulse scheme, the normalized echo signal is given by (*2, 25*)

$$E(\mathbf{q}) = \int\int d\mathbf{r}\,d\mathbf{r}'\,\rho(\mathbf{r})P_s(\mathbf{r}|\mathbf{r}', \Delta) \times \exp(i2\pi\mathbf{q}\cdot\mathbf{r})\exp(-i2\pi\mathbf{q}\cdot\mathbf{r}'), \qquad [1]$$

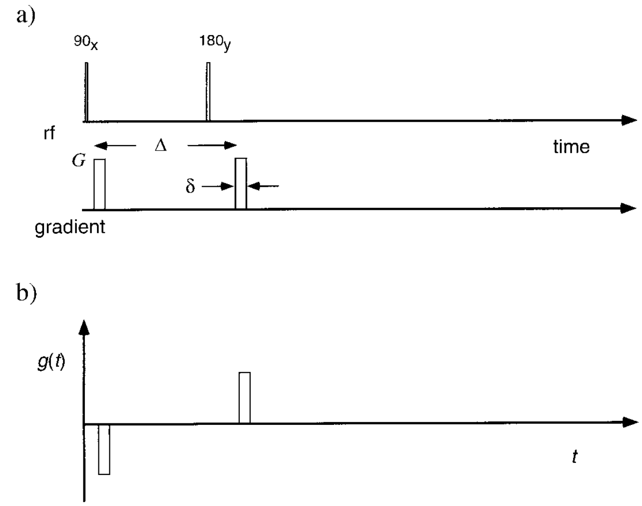

FIG. 1. Representation of (a) a pulse sequence for a standard narrow pulse, PGSE experiment and (b) an effective gradient waveform.

where $\mathbf{q} = (2\pi)^{-1}\gamma\mathbf{G}\delta$, $\rho(\mathbf{r})$ is the probability distribution of starting positions, and $P_s(\mathbf{r}|\mathbf{r}', t)$ is the propagator which gives the probability that a spin starting at position $\mathbf{r}$ will move to $\mathbf{r}'$ at a later time t. Quite apart from its intrinsic Fourier transform properties, the further beauty of Eq. [1] lies in the property that the particle motion is separable from the phase evolution behavior by virtue of the fact that details of the motion reside entirely within the propagator. This propagator language is fundamental to statistical physics and translates directly to other scattering experiment formalisms, for example, inelastic neutron scattering (*2*).

The narrow gradient pulse approximation which underpins the impulse description of Eq. [1] depends on an assumption both that $\delta \ll \Delta$ and that in the case of particles constrained to diffuse within a restricted region of dimension a, $\delta \ll a^2/2D$ where D is the particle self-diffusion coefficient.

GENERALIZED GRADIENT WAVEFORMS AND STOCHASTIC MOTION—THE FREQUENCY DOMAIN

Suppose we consider first the case where the particle motion is simply isotropic unrestricted diffusion (D) under an effective gradient waveform $\mathbf{g}(t)$. In that case the Bloch–Torrey equation (*24*) implies that

$$E(t) = \exp\left[-D\gamma^2\int_0^t\left(\left(\int_0^{t'}\mathbf{g}(t'')dt''\right)^2 dt'\right)\right]. \qquad [2]$$

This equation yields, in the case of the PGSE experiment with two gradient pulses of finite duration, the well-known Stejskal–Tanner formula (*1*)

$$E(q) = \exp(-4\pi^2q^2D(\Delta - \delta/3)). \qquad [3]$$

In the alternative approach to the description of generalized gradient waveforms given by Stepisnik (*26*), the echo attenuation signal is expressed using a spectral density description of motion. In particular it can be shown that the spectrum of translational motion is sampled by relevant spectral components of the time integral of the gradient waveform

$$\mathbf{F}(t) = \gamma \int_0^t \mathbf{g}(t')dt'. \qquad [4]$$

If one allows the random particle migration to be described by a fluctuating velocity $\mathbf{v}_{is}(t)$ the diffusion tensor for the motion can be written as the spectral density of the ensemble-averaged velocity auto-correlation function,

$$D(\omega) = \int_{-\infty}^{\infty} \tfrac{1}{2}\langle \mathbf{v}_{is}(t')\mathbf{v}_{is}(0)\rangle \exp(i\omega t')dt'. \qquad [5]$$

Provided that the signal amplitude is measured at a time such that $\mathbf{F}(t) = 0$ (the usual echo condition), one finds that

$$E(t) = \exp\left(-\frac{1}{\pi}\int_0^{\infty} \mathbf{F}(\omega)D(\omega)\mathbf{F}(-\omega)d\omega\right). \qquad [6]$$

The exponent simplifies, in the case of isotropic diffusion, to $(1/\pi)\int_0^{\infty} D(\omega)|\mathbf{F}(\omega, t)|^2 d\omega$ where the general gradient modulation spectrum, $\mathbf{F}(\omega)$, is given by

$$\mathbf{F}(\omega) = \int_0^t \mathbf{F}(t')\exp(i\omega t')dt'. \qquad [7]$$

Equation [6] depends on an assumption of a Gaussian distribution of spin precession phases. Under the particular condition that the diffusion coefficient is frequency independent (unrestricted Brownian motion) then these equations are consistent with the Bloch–Torrey equation and reproduce the Stejskal–Tanner result in the case of the two-gradient-pulse experiment.

In an earlier paper Callaghan and Stepisnik (*17*) showed that a repetitive CPMG train of RF pulses with interspersed, equally spaced gradient pulses of duration δ and amplitude g produces the nearly ideal frequency sampling function. Under this waveform the echo amplitude is sensitive to the diffusion spectrum at the frequency $2\pi/T$ where T is the period of $\mathrm{F}(t)$. The echo attenuation function after N periods of the waveform is given by

$$E(NT) \approx \exp(-\tfrac{1}{2}NT\gamma^2 G^2\delta^2 D(2\pi/T)). \qquad [8]$$

The Gaussian phase assumption which lies at the heart of the derivation of Eq. [6] is extremely delicate in the case where the particle motion is restricted by collision with reflecting or partially absorbing walls. A satisfactory description of this type of behavior must be a goal of any theoretical treatment dealing with generalized gradient waveforms.

RESTRICTED DIFFUSION AND THE NARROW PULSE PGSE EXPERIMENT

The problem of restricted diffusion is easily handled in the simple two-impulse PGSE experiment, for which the echo attenuation is given exactly by Eq. [1]. Indeed all the physics for the particular problem is contained within the propagator, $P_s(\mathbf{r}|\mathbf{r}', t)$ and the problem reduces, in effect to solving for this distribution. The differential equation governing $P_s(\mathbf{r}|\mathbf{r}', t)$ is Ficks' law,

$$D\nabla'^2 P_s = \partial P_s/\partial t. \qquad [9]$$

This equation may be tackled via the standard eigenmode expansion (*27*)

$$P_s(\mathbf{r}|\mathbf{r}', t) = \sum_{n=0}^{\infty} \exp(-\lambda_n t)u_n(\mathbf{r})u_n^*(\mathbf{r}'), \qquad [10]$$

where the $u_n(\mathbf{r}')$ are an orthonormal set of solutions to the Helmholtz equation parameterized by the eigenvalue λ_n. They are further subject to the identity

$$\delta(\mathbf{r} - \mathbf{r}') = \sum_{n=0}^{\infty} u_n(\mathbf{r})u_n^*(\mathbf{r}'). \qquad [11]$$

P_s, thus constructed, satisfies the initial condition

$$P_s(\mathbf{r}|\mathbf{r}', 0) = \delta(\mathbf{r} - \mathbf{r}'). \qquad [12]$$

The eigenvalues λ_n depend on the boundary condition for the case of relaxing walls, namely (*28*)

$$D\hat{\mathbf{n}}.\nabla P_s + MP_s = 0, \qquad [13]$$

where $\hat{\mathbf{n}}$ is the outward surface normal and M is the usual wall relaxation parameter (*28*). Using these relationships Eq. [1] has been solved exactly in the case of molecules diffusing within parallel planes, cylinders, and spheres, and closed form expressions for these geometries have been derived (*29–32*). What we now seek is a method by which the language of the propagator may be generalized to handle any gradient waveform, and not just the two-impulse experiment depicted in Eq. [1]. One motivation for this approach is to decouple the physics of the restricted diffusion from that of the NMR pulse sequence employed. Ideally we would like a general expression for the echo attenuation which satisfies the following two conditions.

(i) The propagator description should be retained and the nature of the restricted diffusion should be embedded entirely within the mathematical form of that propagator.

(ii) The gradient waveform should appear within a closed form expression in a natural and obvious manner, so that the time sequence of the waveform evolution is explicit.

THE MULTIPLE PROPAGATOR APPROACH

Recently Caprihan *et al.* (*16*) postulated that the case of restricted diffusion under general gradient waveforms could be handled by breaking the gradient pulse into successive intervals and writing a propagator for each stage of the evolution. Their general mathematical expression involved a multiple sum over a large number of independent terms, although they were able to simplify this somewhat in the case of the finite gradient pulse PGSE experiment. Here we adopt a similar philosophy but our derivation differs from that presented by Caprihan *et al.* in that we derive a much simpler, and quite general, closed form expression, and we do so in a manner which demonstrates explicitly the succession of spin phase evolutions at each step of the gradient waveform. These evolutions are expressed in terms of a product of matrix operators between which are sandwiched time evolution terms associated with the diffusive motion. Because of the emergence of Mathematical Tools such as *Matlab,* and *Mathematica,* the matrix product is trivial to evaluate and so the expression presented here provides a practical tool for rapid computation. Furthermore the expression is so straightforward that it can be immediately adapted to any sequence by organizing the matrices as required.

In order to retain the language of propagators when dealing with generalized gradient waveforms, the particulate translational motion must be subdivided into a sequence of discrete time intervals, with all spin phase evolution taking place at well-defined times at the boundaries of those intervals. In other words we will require the narrow pulse approximation of Eq. [1] to apply over each evolutionary step, if not over the entire waveform duration. This means, in effect, that we must approximate the gradient waveform by a succession of impulses, such that the time integral function, $\mathbf{F}(t)$, is represented by a stepwise progression. The basic scheme is shown in Fig. 2. Suppose that we break the waveform into N time intervals τ each bounded by impulses $\mathbf{q}_n$, $\mathbf{q}_{n+1}$, etc. We may discretise the waveform amplitude $\mathbf{g}(n\tau)$ into units of dimension $\mathbf{g}_{\text{step}}$. At time $n\tau$ the impulse will be $\mathbf{q}_n = m_n\mathbf{q}$ where $\mathbf{q} = (2\pi)^{-1}\gamma\delta\mathbf{g}_{\text{step}}$ and m_n is some positive or negative integer, depending on the local magnitude and sign of $\mathbf{g}(n\tau)$ and given by

$$m_n = \text{integ}(\mathbf{g}(n\tau))/\mathbf{g}_{\text{step}}. \quad [14]$$

Thus we may write the echo amplitude at the end of the sequence as

$$\begin{aligned} E = &\int d\mathbf{r}_1 \int d\mathbf{r}_2 \cdots \int d\mathbf{r}_{N+1} \rho(\mathbf{r}_1) \exp(i2\pi\mathbf{q}_1 \cdot \mathbf{r}_1) \\ &\times P_s(\mathbf{r}_1|\mathbf{r}_2, \tau) \exp(i2\pi\mathbf{q}_2 \cdot \mathbf{r}_2) P_s(\mathbf{r}_2|\mathbf{r}_3, \tau) \cdots \\ &\times \exp(i2\pi\mathbf{q}_N \cdot \mathbf{r}_N) P_s(\mathbf{r}_N|\mathbf{r}_{N+1}, \tau) \\ &\times \exp(i2\pi\mathbf{q}_{N+1} \cdot \mathbf{r}_{N+1}). \end{aligned} \quad [15]$$

Using Eq. [10] we find

$$\begin{aligned} E = &\int d\mathbf{r}_1 \int d\mathbf{r}_2 \cdots \int d\mathbf{r}_{N+1} \rho(\mathbf{r}_1) \exp(i2\pi\mathbf{q}_1 \cdot \mathbf{r}_1) \\ &\times \sum_{k_1} u_{k_1}(\mathbf{r}_1) u^*_{k_1}(\mathbf{r}_2) \exp(-\lambda_{k_1}\tau) \exp(i2\pi\mathbf{q}_2 \cdot \mathbf{r}_2) \\ &\times \sum_{k_2} u_{k_2}(\mathbf{r}_2) u^*_{k_2}(\mathbf{r}_3) \exp(-\lambda_{k_2}\tau) \cdots \\ &\times \exp(i2\pi\mathbf{q}_N \cdot \mathbf{r}_N) \cdot \mathbf{r}_N) \sum_{k_N} u_{k_N}(\mathbf{r}_N) u^*_{k_N}(\mathbf{r}_{N+1}) \\ &\times \exp(-\lambda_{k_N}\tau) \exp(i2\pi\mathbf{q}_{N+1} \cdot \mathbf{r}_{N+1}) \end{aligned} \quad [16]$$

$$\begin{aligned} = &\int d\mathbf{r}_1 \int d\mathbf{r}_2 \cdots \int d\mathbf{r}_{N+1} \rho(\mathbf{r}_1) \exp(i2\pi\mathbf{q}_1 \cdot \mathbf{r}_1) \\ &\times \sum_{k_1k_2\cdots k_N} u_{k_1}(\mathbf{r}_1) u^*_{k_1}(\mathbf{r}_2) \exp(-\lambda_{k_1}\tau) \\ &\times \exp(i2\pi\mathbf{q}_2 \cdot \mathbf{r}_2) u_{k_2}(\mathbf{r}_2) u^*_{k_2}(\mathbf{r}_3) \exp(-\lambda_{k_2}\tau) \cdots \\ &\times \exp(i2\pi\mathbf{q}_N \cdot \mathbf{r}_N) u_{k_N}(\mathbf{r}_N) u^*_{k_N}(\mathbf{r}_{N+1}) \\ &\times \exp(-\lambda_{k_N}\tau) \exp(i2\pi\mathbf{q}_{N+1} \cdot \mathbf{r}_{N+1}) \end{aligned} \quad [17]$$

$$\begin{aligned} = &\sum_{k_1k_2\cdots k_N} S_{k_1}(\mathbf{q}_1) R_{k_1k_1} A_{k_1k_2}(\mathbf{q}_2) R_{k_2k_2} A_{k_2k_3}(\mathbf{q}_3) \cdots \\ &\times R_{k_{N-1}k_{N-1}} A_{k_{N-1}k_N}(\mathbf{q}_N) R_{k_Nk_N} S^*_{k_N}(-\mathbf{q}_{N+1}), \end{aligned} \quad [18]$$

where

$$S_k(\mathbf{q}) = V^{-1/2} \int d\mathbf{r}\, u_k(\mathbf{r}) \exp(i2\pi\mathbf{q} \cdot \mathbf{r}) \quad [19]$$

$$R_{kk} = \exp(-\lambda_k\tau) \quad [20]$$

$$A_{kk'}(\mathbf{q}) = \int d\mathbf{r}\, u^*_k(\mathbf{r}) u_{k'}(\mathbf{r}) \exp(i2\pi\mathbf{q} \cdot \mathbf{r}), \quad [21]$$

and we note that the initial density, $\rho(\mathbf{r}_1)$, may be set to the inverse of the pore volume (V) provided that the eigenfunctions are appropriately normalized. We further note via Eq. [11] that

$$A_{kk''}(\mathbf{q}_A + \mathbf{q}_B) = \sum_{k'} A_{kk'}(\mathbf{q}_A) A_{k'k''}(\mathbf{q}_B), \quad [22]$$

from which we obtain the result that $A(n\mathbf{q}) = A(\mathbf{q})^n$.

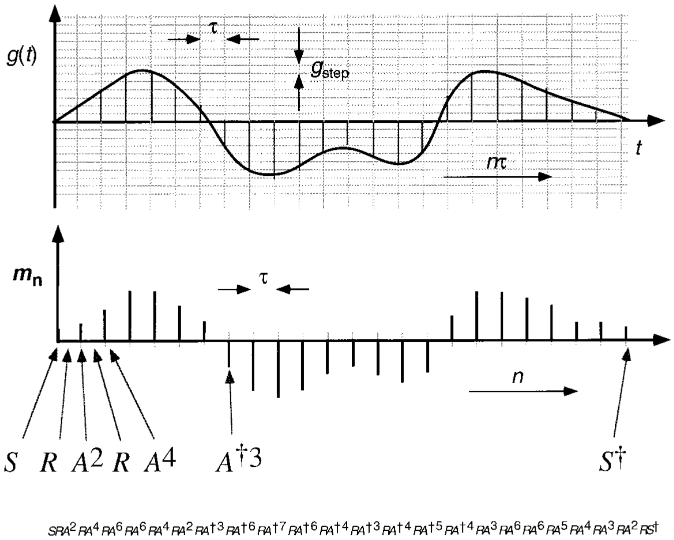

FIG. 2. Schematic decomposition of a generalized gradient waveform into a sequence of equally time-separated impulses, each of whose magnitudes are expressed as integer multiples, m_n, of the basic digitization unit, g_{step}. From this train the succession of matrix operators may be written directly, starting and finishing with the S row and column vectors. The effect of the diffusive evolution is contained within the diagonal R matrices while that of the phase evolutions is contained in the A matrices each of which is raised to the power m_n, the integer corresponding to the impulse strength at the nth step. Negative gradients are represented by using the Hermitian transpose of A. The entire sequence shown is indicated in the matrix product below the diagram.

Hence we may write our echo attenuation scheme using the simple matrix product

$$E = S(\mathbf{q}_1)RA(\mathbf{q}_2)RA(\mathbf{q}_3)\cdots RA(\mathbf{q}_N)RS^{\dagger}(-\mathbf{q}_{N+1}). \quad [23]$$

It is the recognition of the matrix algebra inherent in Eqs. [18] to [23] which represents the key simplifying step in our formulation of the problem. Let us consider the case of a waveform $\mathbf{g}(t)$ which begins and ends with zero amplitude and which has zero time integral at the sampling time in order to satisfy the echo condition. As shown in Fig. 2, we represent this waveform by a series of equally spaced impulses. While this may seem a rather crude approximation in the domain of $\mathbf{g}(t)$, it provides a stepwise approximation to the more important time-integral waveform, $\mathbf{F}(t)$. Setting, for convenience, the initial and final impulses to the minimum value $\mathbf{q}$ (an unimportant requirement if N is sufficiently large) we find that

$$E = S(\mathbf{q})R[A(\mathbf{q})]^{m_2}\cdots \times R[A(\mathbf{q})]^{m_n}\cdots R[A(\mathbf{q})]^{m_N}RS^{\dagger}(-\mathbf{q}). \quad [24]$$

Thus we find that in general, any waveform may be handled, provided that we calculate just three matrices, $R(\tau)$, $S(\mathbf{q})$, and $A(\mathbf{q})$, where $\mathbf{q}$ is the smallest impulse used to digitize the waveform.

EXAMPLES OF E(q) FOR DIFFERENT WAVEFORMS

We now demonstrate the application of Eq. [24] in a number of cases of special interest.

(i) Steady gradient spin echo. The effective gradient is as shown in Fig. 3a. We break the waveform into $2N + 1$ intervals and $2N + 2$ impulses so that the total effective scattering wave vector amplitude is $q_{net} = (N + 1)q$, with

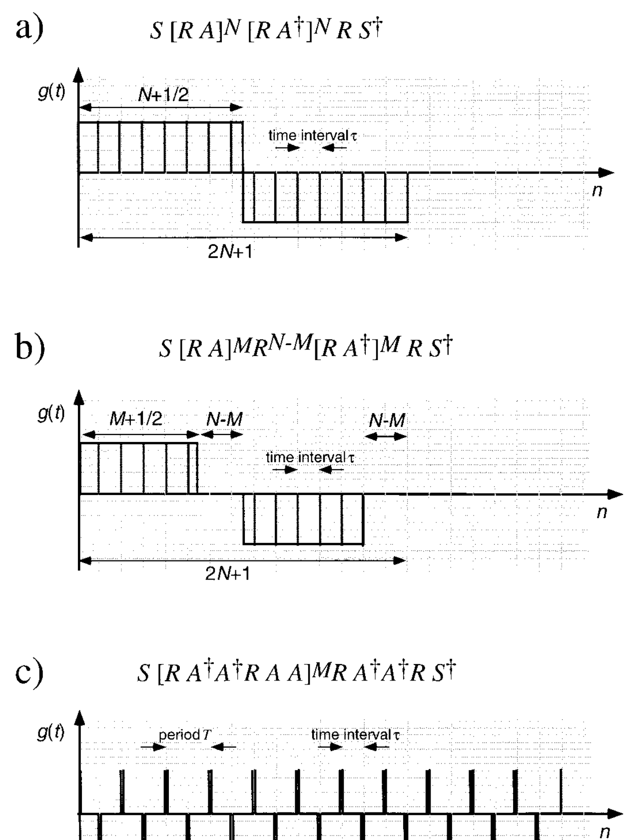

FIG. 3. Schematic illustration of impulse decomposition of three different pulse sequences. The sequences are shown using a small number of impulses simply for clarity. In practice one may calculate the echo attenuation quite rapidly using on the order of 100 impulses. In each case the evolution matrix product corresponding to the sequence is shown above. (a) The steady gradient spin echo (or pulsed gradient spin echo with $\delta = \Delta$) represented by a train of constant magnitude impulses, q. Note that $\Delta = (N + 1/2)\tau$ while the wave vector value corresponding to the area under the complete gradient pulse is $q_{net} = (N + 1)q$. (b) Finite pulse width PGSE experiment in which $q_{net} = (M + 1)q$, $\Delta = (N + \frac{1}{2})\tau$, and $\delta = (M + \frac{1}{2})\tau$. (b) CPMG PGSE sequence in which the time integral effective gradient waveform, $\mathbf{F}(t)$, oscillates as a square wave, thus sampling the diffusional motion in the frequency domain.

the pulse spacing and pulse duration identical and given by $\Delta = (N + \frac{1}{2})\tau$ and $\delta = (N + \frac{1}{2})\tau$ respectively:

$$E = S(q)[RA(q)]^N[RA^\dagger(q)]^N RS^\dagger(q). \quad [25]$$

Note that the final and initial impulses have opposite sign q amplitudes so that for this case the initial and final vectors are respectively $S(\mathbf{q}_1) = S(q)$, and $S^\dagger(-\mathbf{q}_{2N+2}) = S^\dagger(q)$.

(ii) Finite gradient pulse spin echo. The effective gradient is as shown in Fig. 3b. In this case we break the entire waveform into $2N + 1$ intervals so that the total effective scattering wave vector amplitude is $q_{\text{net}} = (M + 1)q$, with $\Delta = (N + \frac{1}{2})\tau$ and $\delta = (M + \frac{1}{2})\tau$. Here we find that

$$E = S(q)[RA(q)]^M R^{N-M}[RA^\dagger(q)]^M RS^\dagger(q). \quad [26]$$

Note that in the narrow gradient pulse approximation $M = 0$, and we have

$$E = S(q)R^{N+1}S^\dagger(q). \quad [27]$$

From Eqs. [10] and [19] we see that this form is precisely consistent with Eq. [1]. Furthermore Eq. [27] may be identified as the sum

$$E = \sum_{k=0}^{\infty} |S_k(q)|^2 \exp(-\lambda_k\Delta), \quad [28]$$

where $S_k(q)$ is the spectral component of the phase factor, $\exp(i2\pi\mathbf{q}\cdot\mathbf{r})$, expressed in the basis of eigenkets $\{u_k^*(\mathbf{r})\}$, i.e.,

$$\exp(i2\pi\mathbf{q}\cdot\mathbf{r}) = \sum_{k=0}^{\infty} S_k(q)u_k^*(\mathbf{r}). \quad [29]$$

Equation [28] illustrates that the echo attenuation is given by a superposition of damped structure factors relating to differing harmonics of the basis set, a result also pointed out by Stepisnik (*21*). With increasing diffusion time the factors from the higher harmonics disappear leaving the lowest order term alone as $\Delta \to \infty$. In this limit E reduces to $|S_0(q)|^2$, the Fourier structure factor of the pore.

(iii) CPMG spin echo train. Consider the effective gradient train shown in Fig. 3c. It comprises $2N$ impulses and N periods of the gradient time integral waveform. This series of impulses may be represented by the relation

$$E = S(q)[RA^\dagger(q)A^\dagger(q)RA(q)A(q)]^M \times RA^\dagger(q)A^\dagger RS^\dagger(-q), \quad [30]$$

where $M = N - 1$. This train, which is slightly different from that originally demonstrated by Callaghan and Stepisnik (*17*), has a square wave time-integral waveform with period $T = 2\tau$ where τ is the time evolution step interval. Here the final and initial impulses have equal sign so that in this case the initial and final operators are respectively $S(\mathbf{q}_1) = S(q)$ and $S^\dagger(-\mathbf{q}_{2N+2}) = S^\dagger(-q)$.

(iv) Sinusoidal gradient train. This waveform can be expressed by using by digitized envelope function expressed by N impulses being integer multiples of g_m at time spacing τ and period $N\tau$, and persisting for P cycles

$$E = S(q)[\prod_{m=1}^{N} RA(q)^{g_m}]^P RS^\dagger(q), \quad [31]$$

where $g_m = \text{integ}(G_m \sin(2\pi m/N))$ and $G_m = \text{integ}(\mathbf{g}_{\max}/\mathbf{g}_{\text{step}})$.

SYMBOLIC INTERPRETATION SCHEME AND COMPUTATIONAL IMPLEMENTATION

The pattern for writing down the matrix product should now be apparent. The product begins and ends with the S row and column vectors while the interior of the product is a sandwich of R and A matrix operators. The time evolution associated with diffusion is contained within $R(\tau)$ while the phase evolution associated with the gradient impulse is embedded in the $A(q)$ matrix. However, both R and A depend on the propagator characteristics through the eigenfunction expansion. To obtain the echo attenuation expression one need simply subdivide the time sequence into a large number of steps (e.g., 100), represent the gradient waveform by an equally spaced impulse train, and then write down the time succession of matrix operators.

In each of the above examples, the S, A, and R matrices are calculated from the eigenfunction expansion relevant to the geometry at hand. We shall give an example of this procedure below. This calculation, and the evaluation of the matrix product can be performed very rapidly by means of the matrix-handling package, *Matlab.* Indeed the speed of this software is such that Eqs. [24] to [28] represent effectively analytic closed form expressions which can be evaluated in seconds with just a few lines of *Matlab* code. For example, using *Matlab* on a Power Macintosh, $E(q)$ at 50 different values of q can be evaluated in a few seconds using up to 100 15×15 matrices in the product. As a consequence the entire time interval can be quite finely subdivided and the validity of the assumptions behind the impulse-propagator formalism can be assured.

Restricted Diffusion between Planes

We now test the relationships derived above in three of the four examples, using as a platform the case of restricted diffusion along the axis normal to two parallel reflecting planes spaced by a distance a. To evaluate Eqs. [25] to [28] for the case of restricted diffusion, we need to obtain the matrix elements of S, R, and A using the fundamental eigenfunction expansion for the particular geometry under study. The required dimension of these matrices will be determined by the exponents of the elements of the R matrix, since we wish the matrix elements sums to converge when multiplying out the products. For $k \times k$ matrices the R matrix elements will decay as $\exp(-k^2\pi^2 D\tau/a^2)$. Provided $k^2 D\tau/a^2 \gg 1$, this condition should be reasonably satisfied, and we have found 15×15 matrices sufficiently accurate for our purposes.

For the planar boundary case, the eigenfunction solutions with and without relaxation at the boundary are well known (*16, 29–32*). We shall consider the case of perfectly reflecting walls but we note that the extension to the partially absorbing case is trivial. For reflecting wall at $z = 0$, a we have

$$u_0 = (1/a)^{1/2} \tag{32a}$$

$$u_k = (2/a)^{1/2}\cos(k\pi z/a) \quad k \neq 0 \tag{32b}$$

$$S = BS' \tag{32c}$$

$$A = C^{\dagger}A'C \tag{32d}$$

$$R = \exp(-k^2\pi^2 D\tau/a^2), \tag{32e}$$

where B and C are diagonal matrices with $B_{00} = 1/a$, $B_{kk} = 2^{1/2}/a$ for $k \neq 0$ and $C_{00} = (1/a)^{1/2}$, $C_{kk} = (2/a)^{1/2}$ for $k \neq 0$ and

$$S'_k = i2a\exp(i\pi qa)(2\pi qa)\cos(\pi qa)/((2\pi qa)^2 - (k\pi)^2) \quad k \neq 0 \text{ odd}$$

$$2a\exp(i\pi qa)(2\pi qa)\sin(\pi qa)/((2\pi qa)^2 - (k\pi)^2) \quad k \neq 0 \text{ even} \tag{33}$$

and

$$A_{kk'} = \tfrac{1}{2}[S'_{|k-k'|} + S'_{k+k'}]. \tag{34}$$

(i) Finite gradient pulse spin echo, steady gradient, and impulse pair gradient. In order to verify our theory we begin by taking Eq. [26], the result for the finite gradient pulse PGSE experiment. Computational evaluations of this problem have been provided by Blees (*15*), who found a numerical solution to the magnetization diffusion equation under the known boundary conditions, and independently by Coy and Callaghan (*6, 33*) using Monte Carlo simulation of particle diffusion. A later Monte Carlo computer simulation has also been carried out by Linse and Söderman (*34*).

We now compare the results of the analytic theory with all three sets of numerical ''data,'' in each case using discrete points taken from the published simulations and comparing these with solid lines from the theory. First, we have calculated $E(q)$ using Eq. [26] and under identical conditions to those used in the Monte Carlo simulations of Coy and Callaghan (*6*), namely $\Delta = 0.6\ a^2/D$ with $\delta = \Delta/8$, $\Delta/4$, $\Delta/2$ and the steady gradient case, $\delta = \Delta$. The comparison is shown in Fig. 4 where the agreement is excellent. As required we also find that the infinitesimal gradient pulse

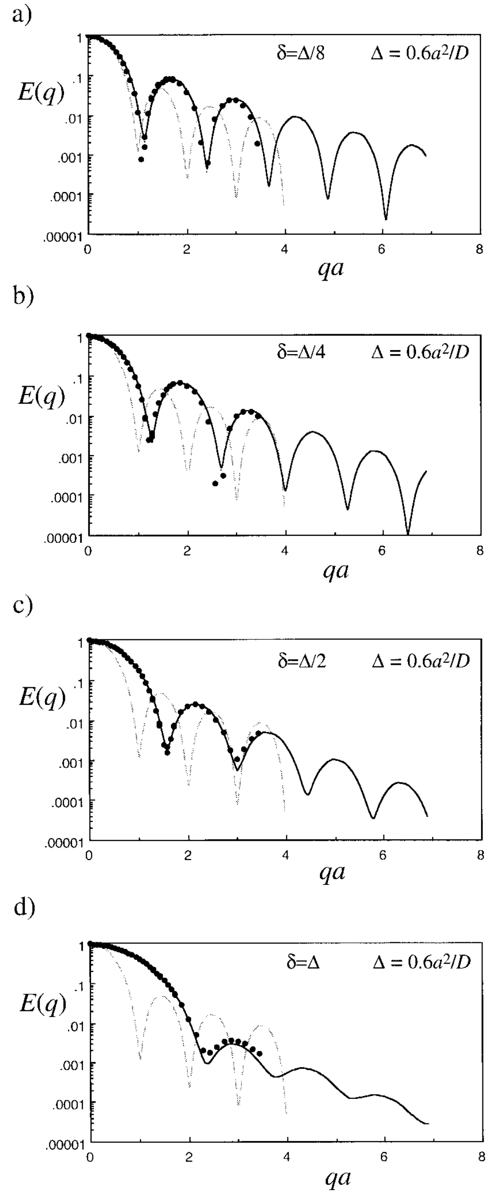

FIG. 4. Comparison of the impulse-propagator theory with Monte Carlo simulations of finite pulse width PGSE attenuation for the case of restricted diffusion between parallel planes of spacing a. No parameters have been adjusted and the comparison is absolute. The solid line shows the result calculated using Eq. [26] while the dots are the simulation data of Coy and Callaghan (*6*). The dashed curve in each case shows, for reference, the theoretical attenuation for an infinitesimal width gradient pulse. (a–d) show the effect of varying the pulse width duration.

equation [27] agrees precisely with earlier published results (*32*). In Fig. 5 we compare the results of Eq. [26] with the numerical results of Blees at $\Delta D/a^2 = 0.25$, 0.5, and 1.0, at two different values of δ, namely that corresponding to $\delta = 0.5\Delta$, and the extreme limit of constant gradient, $\delta = \Delta$. The infinitesimal gradient pulse limit is also shown. Note that we have retained the differing logarithmic scales used by Blees so that our results may be directly compared with his plots.

It is apparent in Figs. 4 and 5 that the position of the first minimum in $E(q)$ moves to higher values of q as the pulse duration is increased. This shift has been remarked on by a number of authors (*6, 14–16*) and its physical origin can be found in the narrowing in the effective well size by virtue of collisions of molecules with the boundaries, a point which has been nicely explained by Mitra and Halperin (*14*). The Blees and the Coy and Callaghan results for steady gradient ($\delta = \Delta$) are completely consistent and exhibit diffraction first minima at around $qa \approx 2.1$ for $\Delta = 0.5\ a^2/D$, $qa \approx 2.5$ for $\Delta = 0.6a^2/D$, and $qa \approx 3.3$ for $\Delta = a^2/D$. A highly significant finding is that we verify, for the case of the maximum pulse duration $\delta = \Delta$, the substantial shift of the diffraction minimum as the diffusion length, $D\Delta/a^2$, increases, with no asymptotic limit being evident. This result stands in contrast to the predictions of the approximate ''structure waves discord'' theory of Stepisnik (*21, 35*).

Finally we show in Fig. 6 the comparison of the predictions of Eq. [26] with the simulations by Linse and Söderman, for the cases $\Delta D/a^2 = 0.2$, 0.5, and 1.0. The parameters used in Fig. 6 are identical to those used in their Fig. 4d, namely $\gamma G = 40D/a^3$ and $200D/a^3$. At first sight, the Linse and Söderman simulation for $\Delta = 0.5a^2/D$ appears very different from that shown in Refs. (*6, 15*), since the minimum occurs at $qa \approx 1.5$. However it must be appreciated that these authors performed their analysis of $E(q)$ by keeping the gradient amplitude, G, constant and varying the duration of the gradient pulse. As a consequence their minimum corresponds to a point where $\delta = 0.47\Delta$. Both Blees and Coy and Callaghan find $qa \approx 1.5$ for $\delta = 0.5\Delta$ so that all the numerical analyses which have been published are quite consistent.

Note that in all the comparisons shown here there are no adjustable parameters. The comparisons shown in Figs. 4, 5, and 6 are absolute. The excellent agreement of the predictions of Eq. [26] with all three sets of simulations serves to illustrate the satisfactory nature of the analytic theory, while at the same time emphasizing the consistency between the three independent sets of numerical analyses.

We emphasize again that the multiple propagator approach was also used by Caprihan *et al.* to find echo attenuations for the finite gradient pulse experiment. These authors compared the position of the first $E(q)$ minimum with that found by Blees. While our fundamental methodology is derived from that earlier work, our own result differs from

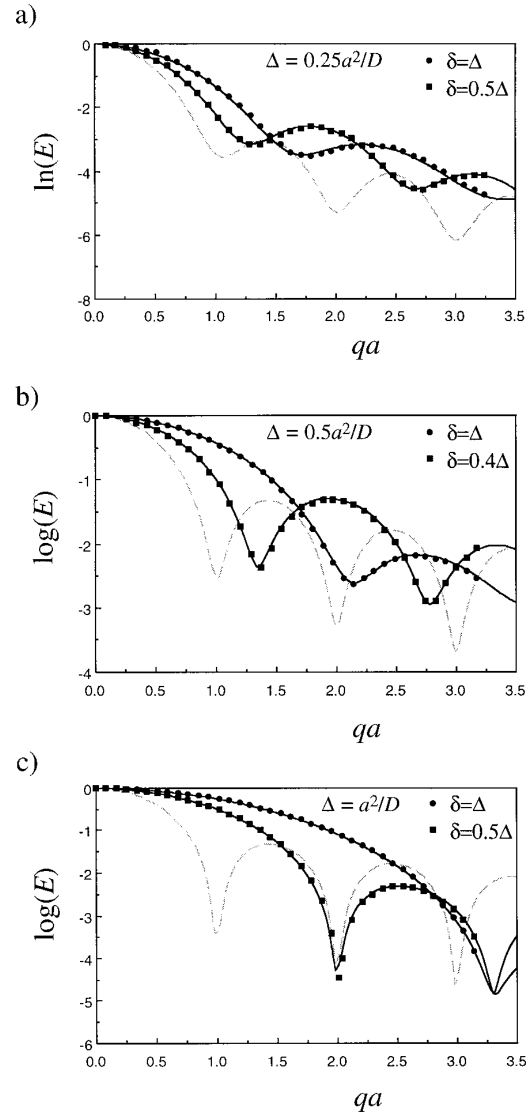

FIG. 5. As described in the legend to Fig. 4 but the predictions of Eq. [26] are compared absolutely with the data of Blees (*15*) (dots and squares). Unlike the Monte Carlo data shown in Fig. 4, the values of Blees were obtained by numerical solution to the magnetization diffusion equation. Note the dramatic shift in diffraction minimum for $\delta = \Delta$ as the diffusion length is increased from (a) 0.25 to (c) 1.0. Note also that in (a) the ordinate scale is $\log_e$ while in (b, c) it is $\log_{10}$, in accordance with those used originally in Ref. (*15*).

the Caprihan *et al.* paper in the extreme simplicity of our attenuation formula, as evident in Eq. [26], and in the comprehensive test of the result against all available simulations and across the entire q range of the echo attenuation plots.

Figure 7a shows the results of echo attenuation calculations carried out for the steady gradient case (Eq. [25]) over a range of values of $D\Delta/a^2$ from 0.1 to 0.01, this time plotted as a conventional Stejskal–Tanner plot in recognition of the Gaussian character of the echo attenuation at short diffusion times. The plots asymptotically approach the free

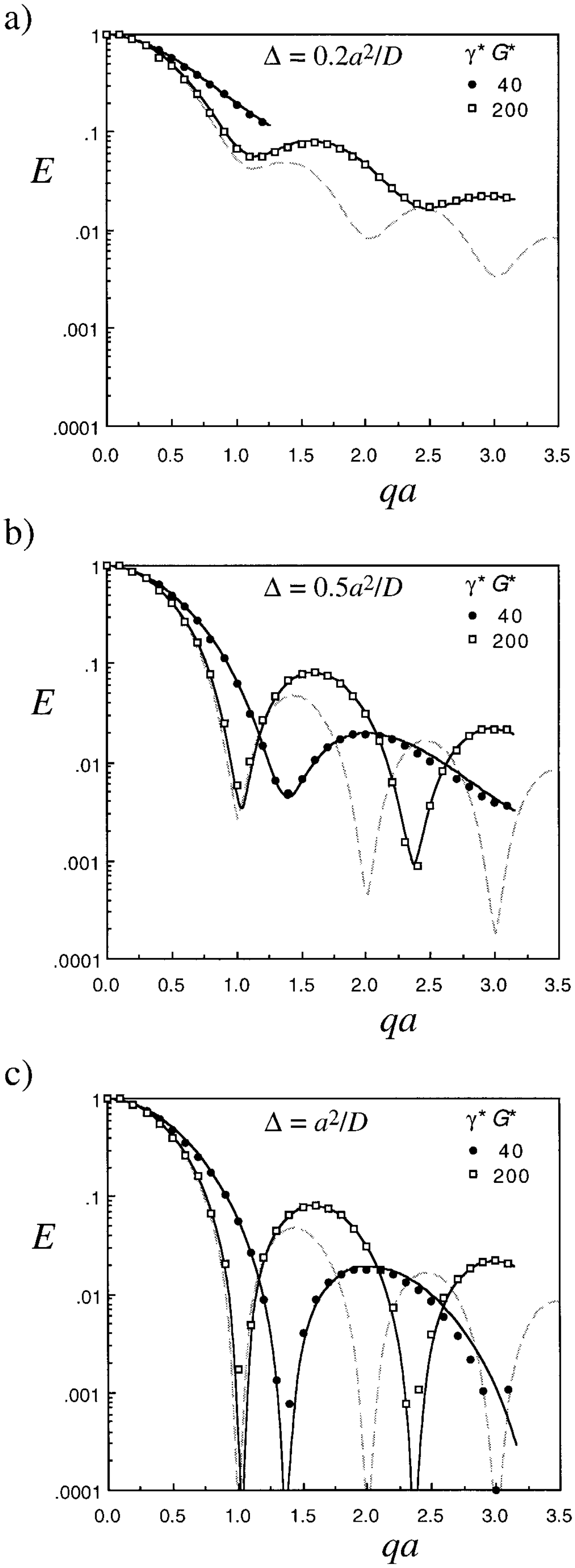

FIG. 6. As described in the legend to Fig. 4 but in which the predictions of Eq. [26] are compared absolutely with the Monte Carlo simulations of Linse and Soderman (*34*). By contrast with the data shown in Figs. 4 and 5, the q values are changed by changing the duration of the gradient pulse, keeping the gradient amplitude constant (●, $\gamma G = 40D/a^3$, and □, $200D/a^3$). Again the diffusion length is varied from (a) 0.2 to (c) 1.0. The reason that no dramatic shift in the diffraction minimum is apparent in (c) is due to the fact that δ is significantly less than Δ in this diagram. These data are in fact completely consistent with those of Blees and of Coy and Callaghan.

diffusion limit of unity slope as $D\Delta/a^2 \ll 1$. At finite values of Δ the reduced effective diffusion coefficient manifests the boundary attenuation phenomenon outlined by Mitra and co-workers (*36*), in which a layer of fluid of thickness on the order of $(D\Delta)^{1/2}$ has impeded diffusion.

(ii) The effective wavevector for the finite gradient pulse. Note that Eq. [28], when evaluated for the case of the parallel plates, returns the long time limit single slit diffraction result as required:

$$E = |S_0(q)|^2 = \left|\frac{\sin(\pi qa)}{\pi qa}\right|^2. \qquad [35]$$

For a finite duration gradient pulse we can define an effective scattering wavevector, q_{eff}, such that the position of the diffraction minimum is that given by a narrow pulse experiment with this wavevector. In other words

$$S(q)[RA(q)]^M R^{N-M}[RA^\dagger(q)]^M RS^\dagger(q) = S(q_{\text{eff}})R^{N_{\text{eff}}}S^\dagger(q_{\text{eff}}), \qquad [36]$$

where $N_{\text{eff}}\tau$ is the effective sharp pulse separation, Δ_{eff}. In order to identify $S(q_{\text{eff}})$ we rewrite the left-hand side of Eq. [36] as $S(q)[RA(q)]^M R^L R^{N_{\text{eff}}} R^L [RA^\dagger(q)]^M RS^\dagger(q)$, where $L = (N - M - N_{\text{eff}})/2$. Thus we find that

$$S(q_{\text{eff}}) \approx S(q)[RA(q)]^M R^L. \qquad [37]$$

Thus q_{eff} and Δ_{eff} are interdependent. We may however define q_{eff} by taking the lowest order structure factor $|S_0(q_{\text{eff}})|^2$ where $S_0(q_{\text{eff}})$ is the $k = 0$ element of the vector, $S(q)[RA(q)]^M$. Note that in this limit, the term R^L in Eq. [37] has no influence, as is to be expected given that the lowest order term corresponds to the long time limiting case for two narrow gradient pulses. We have used the right-hand side of Eq. [37] to generate lowest order structure factors (diffraction patterns) for E over a wide range of finite width gradient pulses at finite diffusion times and always find that q_{eff}, as defined by the first minimum of $|S_0(q_{\text{eff}})|^2$, coincides precisely with the position of the first minimum of E.

(iii) CPMG spin echo train. We now consider a completely different pulse train for which there exists no known solution for the echo attenuation under conditions of restricted diffusion. This is the periodic train of Fig. 3c, the basis of the FD-MGSE experiment of Callaghan and Stepis-

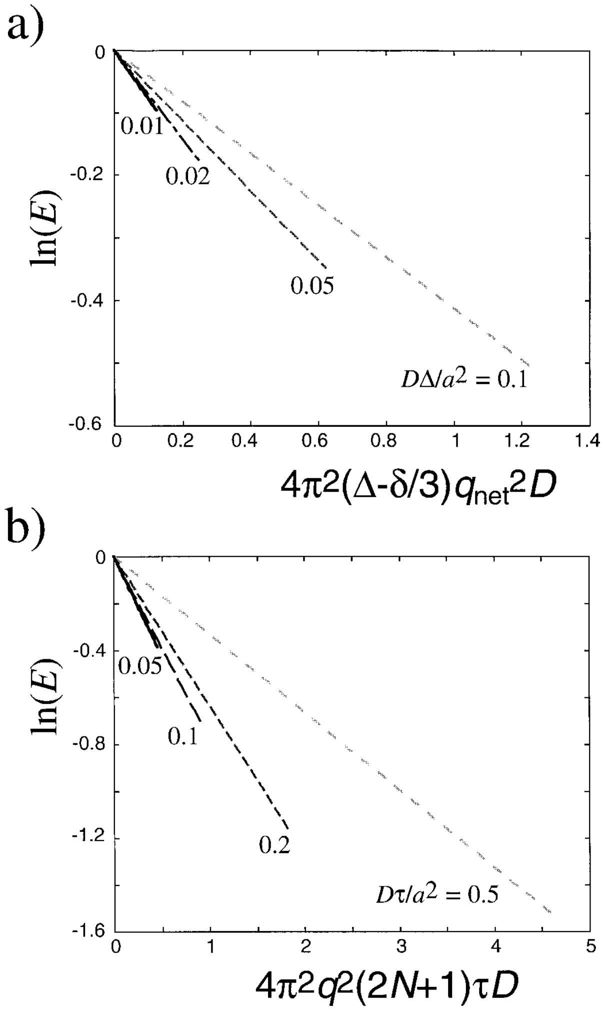

FIG. 7. (a) Stejskal–Tanner echo attenuation plot for the finite width PGSE experiment at small diffusion lengths where the data are approximately Gaussian. The asymptotic trend to free diffusion is apparent as the diffusion length decreases. Note that $q_{\mathrm{net}} = q(N+1)$. (b) Echo attenuation plot for the CPMG FD-MGSE experiment, plotted according to Eq. [39] so that the slope yields the ratio D_{app}/D. By contrast with the two-pulse PGSE experiment, the relevant diffusion length scale is determined by the much shorter oscillation period, 2τ, rather than the sequence duration. Again, the asymptotic trend to free diffusion is apparent as the diffusion length decreases, with the relevant time being the period $T = 2\tau$, rather than the total pulse train duration.

nik (*17*). For unrestricted diffusion we can write down the expected echo attenuation very simply. A single pair of impulses with wave vector q separated by τ will contribute $\exp(-4\pi^2 q^2 D\tau)$. For N periods of the waveform we have $(2N+1)$ pairs in succession, leading to

$$E(NT) = \exp(-4\pi^2 q^2 (2N+1) D\tau) \qquad [38]$$

The interesting question concerns the behavior of the echo attenuation under restricted diffusion as the pulse spacing τ is varied. This series of impulses is ideally represented by the formalism of this article, and we may calculate the resulting echo signal for any number of pulses via Eq. [30]. Figure 7b shows the result of a series of calculations made for $N = 100$ for a range of values of $D\tau/a^2$, in which the logarithm of the echo attenuation is plotted against q^2. The linearity of all these plots attests to Gaussian behavior over all time scales. Such Gaussian behavior, despite the restriction of free diffusion, results from the cumulative effect of many small phase excursions and is a consequence of the central limits theorem. Hence we may rewrite Eq. [38] to define an apparent diffusion coefficient *via*

$$E(NT) = \exp(-4\pi^2 q^2 (2N+1) D_{\mathrm{app}}\tau). \qquad [39]$$

As in the case of the steady gradient train the asymptotic behavior is apparent, but this time governed by the $D\tau/a^2$ criterion rather than the $D\Delta/a^2$ criterion. The echo attenuation experienced under this periodic waveform is also dramatically less than experienced in the steady gradient case over the same total period, as is to be expected, given the oscillatory behavior of the gradient time integral, $\mathbf{F}(t)$. This can be seen in Fig. 7 by noting that $q_{\mathrm{net}} = q(N+1)$ so that the abscissa scales in Figs. 7a and 7b differ by a factor of order N.

In Fig. 7b we see the effect of restricted diffusion over the time scale τ separating the pulses in the CPMG train. Using these results for the $E(q)$ along with Eq. [39], we can calculate the apparent diffusion coefficient by linear regression. For the smallest values, the value of D_{app}/D returned from a linear regression is around unity, but once $D\tau/a^2$ approaches 1, the apparent diffusion coefficient drops. Figure 8 shows the normalized apparent diffusion coefficient as a function of frequency, $1/2\tau$. Because the gradient waveform samples the translational motion spectral density so strongly at the fundamental frequency $1/2\tau$, we may view this graph as a measure of the diffusion spectrum for this problem, and, as has been noted earlier (*17, 18*), because the waveform can easily be applied with spacings of less than 1 ms, we are able to probe this density up to kilohertz frequencies. The generalization of this approach to other problems involving particle dynamics represents an attractive outcome of the present model.

CONCLUSION

The analysis presented here provides a completely general way to deal with the problem of restricted diffusion under any gradient waveform. Provided one can obtain an eigenfunction expansion for the propagator, the S, R, and A matrices can be evaluated and solution for $E(q)$ may be written down directly. In the present work we have demonstrated solutions for two different waveforms in the case of the parallel plate restricted diffusion problem. Eigen-expansions are also known for the spherical and cylindrical pore geome-

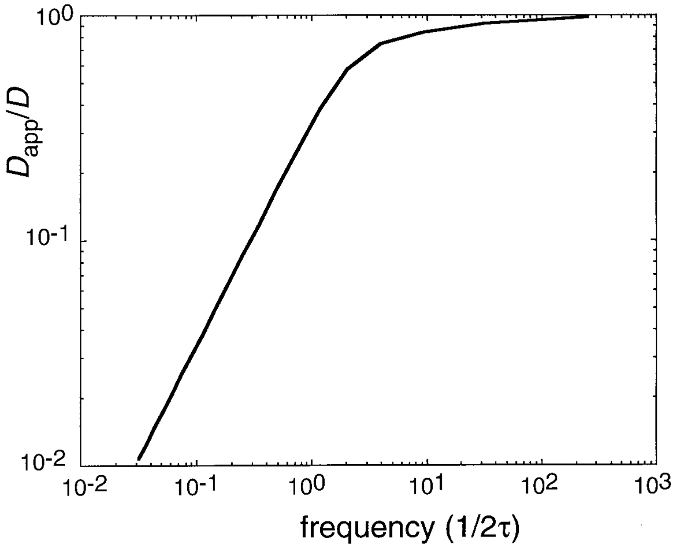

FIG. 8. Spectral density plot of relative apparent diffusion coefficient (given by the slope in Fig. 7b) vs the CPMG frequency $1/2\tau$. (Note that the frequency scale is in units of D/a^2). A clear transition is apparent when $1/T \approx D/a^2$, thus showing the potential of this method to probe restricted diffusion at time and length scales much shorter than those which are accessible in two-pulse PGSE NMR.

tries and all of these incorporate wall relaxation effects (*32*) if desired. Given the fundamental importance of these three cases to the physics of restricted diffusion, the great utility of the current methodology becomes apparent.

As regards to the finite gradient pulse width problem in PGSE NMR, the expression presented here provides a considerable simplification over previous analyses, avoids the need for Monte Carlo simulation or numerical solutions to the diffusion equation, and makes accessible the ready calculation of echo attenuation expressions in a few lines of *Matlab* code. The author is able to provide this code via the internet on P.Callaghan@massey.ac.nz. The implications of this approach for the new method of frequency-domain modulated gradient NMR are considerable. This method has the potential to study restricted diffusion at much smaller time and length scales than previously accessible to two-pulse PGSE NMR, and the new theory presented here should considerably aid the application of this method. Taken together with the alternative insight presented by Stepisnik in a forthcoming article (*35*), the calculation methods now available to experimenters should greatly widen the problems which may be studied as well as the range of gradient modulation techniques which might be applied.

ACKNOWLEDGMENTS

The author acknowledges very stimulating discussions with Professor Janez Stepisnik, both during his sabbatical visit at Massey University, and subsequently at the 28th Ampere Congress 1996. Thanks are also due to Karen Owens who extracted discrete points from published simulations. The financial support of the New Zealand Foundation for Research Science and Technology is also gratefully acknowledged.

REFERENCES

1. E. O. Stejskal and J. E. Tanner, *J. Chem. Phys.* **42,** 288 (1965).
2. P. T. Callaghan, "Principles of Nuclear Magnetic Resonance Microscopy," Oxford Univ. Press, Oxford/New York (1991).
3. D. G. Cory and A. N. Garroway, *Magn. Reson. Med.* **14,** 435 (1990).
4. P. T. Callaghan, A. Coy, D. MacGowan, K. J. Packer, and F. O. Zelaya, *Nature* **351,** 467 (1991).
5. P. T. Callaghan, A. Coy, T. J. P. Halpin, D. MacGowan, K. J. Packer, and F. O. Zelaya, *J. Chem. Phys.* **97,** 651 (1992).
6. A. Coy and P. T. Callaghan, *J. Chem. Phys.* **101,** 4599 (1994).
7. A. Coy and P. T. Callaghan, *J. Colloid Interface Sci.* **168,** 373 (1994).
8. B. Balinov, O. Soderman, and J. C. Ravey, *J. Phys. Chem.* **98,** 393 (1994).
9. P. W. Kuchel, A. J. Lennon, and C. Durrant, *J. Magn. Reson. B* **112,** 1 (1996).
10. P. W. Kuchel and A. J. Lennon, *J. Magn. Reson. A* **111,** 205 (1994).
11. B. P. Hills and J. E. M. Snaar, *Mol. Phys.* **76,** 979 (1992).
12. M. D. King, J. Houseman, S. A. Roussel, N. van Bruggen, S. R. Williams, and D. G. Gadian, *Magn. Reson. Med.* **32,** 707 (1994).
13. O. Soderman and B. Jonsson, *J. Magn. Reson. A* **117,** 94 (1995).
14. P. P. Mitra and B. I. Halperin, *J. Magn. Reson. A* **113,** 94 (1995).
15. M. H. Blees, *J. Magn. Reson. A* **109,** 203 (1994).
16. A. Caprihan, L. Z. Wang, and E. Fukushima, *J. Magn. Reson. A* **118,** 94 (1996).
17. P. T. Callaghan and J. Stepisnik, *J. Magn. Reson. A* **117,** 118 (1995).
18. P. T. Callaghan and J. Stepisnik, *Adv. Magn. Opt. Reson.* **19,** 326 (1996).
19. J. Stepisnik, *Physica B* **104,** 350 (1981).
20. J. Stepisnik, *Prog. NMR Spectrosc.* **17,** 187 (1985).
21. J. Stepisnik, unpublished abstract, 28th Ampere Congress 1996, Canterbury, UK.
22. H. Y. Carr and E. M. Purcell, *Phys. Rev.* **94,** 630 (1954).
23. T. L. James and G. G. McDonald, *J. Magn. Reson.* **11,** 58 (1973).
24. H. C. Torrey, *Phys. Rev.* **104,** 563 (1956).
25. E. O. Stejskal, *J. Chem. Phys.* **43,** 3597 (1965).
26. J. Stepisnik, *Physica B* **198,** 299 (1994).
27. G. Arfken, "*Mathematical Methods for Physicists,*" Academic Press, New York (1970).
28. K. R. Brownstein and C. E. Tarr, *Phys. Rev.* **19,** 2446 (1979).
29. J. E. M. Snaar and H. Van As, *J. Magn. Reson. A* **102,** 318 (1993).
30. P. P. Mitra and P. N. Sen, *Phys. Rev. B Condens. Matter* **45,** 143 (1992).
31. P. P. Mitra, P. N. Sen, and L. M. Schwartz, *Phys. Rev. B* **47,** 8565 (1993).
32. P. T. Callaghan, *J. Magn. Reson. A* **113,** 53 (1995).
33. A. Coy, Ph.D. thesis (unpublished), Massey University, New Zealand, 1994.
34. P. Linse and O. Soderman, *J. Magn. Reson. A* **116,** 77 (1995).
35. J. Stepisnik, *J. Magn. Reson.,* to be published.
36. P. P. Mitra, P. N. Sen, L. M. Schwartz, and P. LeDoussal, *Phys. Rev. Lett.* **68,** 3555 (1992).